Available online at www.sciencedirect.com
SCIENCE DIRECT®
Journal of Power Sources 139 (2005) 44–54
JOURNAL OF POWER SOURCES
www.elsevier.com/locate/jpowsour

Carbon-supported Pt–Ru catalysts prepared by the Nafion stabilized alcohol-reduction method for application in direct methanol fuel cells

Loka Subramanyam Sarma, Tzu Dai Lin, Yin-Wen Tsai, Jium Ming Chen, Bing Joe Hwang*

Nanoelectrochemistry Laboratory, Department of Chemical Engineering, National Taiwan University of Science and Technology, Taipei 106, Taiwan, ROC

Received 12 May 2004; accepted 15 July 2004
Available online 17 September 2004

Abstract

The Nafion stabilized alcohol-reduction method has been used to prepare Pt–Ru catalysts supported on Vulcan XC-72. The particle size and morphology of catalysts are determined by X-ray diffraction analysis and transmission electron microscopy. Well-dispersed catalysts with particle sizes from 3 to 7 nm are achieved. The catalytic activities of these catalysts towards methanol electro-oxidation are investigated at electrode potentials of interest for fuel cells. The addition of Nafion during catalyst preparation enhances the methanol electro-oxidation activity even for low methanol concentrations. The in-house prepared Pt–Ru/C catalysts (MEC-01 and MEC-03) in 0.5 M H_2SO_4 with 5% methanol at 40 °C display a higher catalytic activity than a standard Pt–Ru/C (E-TEK 40) catalyst. In 5% methanol, the impedance of the in-house catalyst is lower than that of the standard Pt–Ru/C (E-TEK 40) catalyst, viz., 26.18 mg Ω versus 139.49 mg Ω. The Structure of the in-house prepared MEC-01 catalyst is compared with that of commercial E-TEK 40 by means of X-ray absorption spectroscopy. The X-ray absorption near-edge (XANES) of the MEC-01 catalyst at Pt L_{III}-edge shows significant variation in white line intensity compared with that of the commercial E-TEK 40 catalyst.

Keywords: Carbon-supported Pt–Ru catalyst; Alcohol-reduction; Impedance; Direct methanol fuel cell

1. Introduction

Direct methanol fuel cells (DMFCs) have been the subject of great interest in the recent years due to their potential application in electric vehicles and as portable power sources [1–12]. Although several electrocatalysts have been employed for the oxidation of methanol [13–18], Pt is the preferred anode catalyst. The formation of CO on the catalyst surface blocks the active sites for CH_3OH oxidation. Therefore, to achieve a reasonable reaction rate, catalysts with lower overpotentials towards methanol oxidation are required. In recent years, Pt–Ru alloys have received renewed attention as the most active anode catalysts for DMFCs [19–25]. The use of Pt alloys is based on the fact that the less noble metal forms the hydrated oxides necessary to oxidize CO at lower potentials. Thus, the CO adsorbed on Pt is oxidized by the second metal through a so-called bifunctional mechanism [26,27], i.e.,

$$\mathrm{Ru} + \mathrm{H_2O} \rightarrow \mathrm{Ru-OH} + \mathrm{H^+} + \mathrm{e^-} \quad (1)$$

$$\mathrm{Pt-CO} + \mathrm{Ru-OH} \rightarrow \mathrm{Pt} + \mathrm{Ru} + \mathrm{CO_2} + \mathrm{H^+} + \mathrm{e^-} \quad (2)$$

The Pt–Ru catalyst is supported on a high-surface-area carbon support such as Vulcan XC-72 in order to achieve high dispersion. Several techniques have been used to prepare the catalysts, such as colloidal chemistry methods [28–32], an impregnation method [33–37], and a reverse micelles method [38,39]. Recently, an alcohol-reduction procedure has been developed for producing Pt–Ru/C catalysts for polymer electrolyte fuel cells [40]. The prepared metal colloids were stabilized with a surfactant dodecyldimethyl (3-sulfo-propyl) ammonium hydroxide (SB12) during the reduction process without influencing the deposition of the colloids on the

* Corresponding author. Tel.: +886 2 27376624; fax: +886 2 27376644.
E-mail address: bjh@ch.ntust.edu.tw (B.J. Hwang).

0378-7753/$ – see front matter © 2004 Elsevier B.V. All rights reserved.
doi:10.1016/j.jpowsour.2004.07.016

Table 1
Preparation conditions for various Pt–Ru/C catalysts

Catalyst	Vulcan XC-72 pretreated	Procedure conditions					
		pH	Stir time (h)	Reducing agent (ml)	Nafion (μL)	Temperature (°C)	Reflux time (h)
MEC-01	HNO_3	11	4	15	1716	70	5
MEC-02	HNO_3	11	4	25	1716	70	5
MEC-03	HNO_3	11	4	35	1716	70	5
MEC-04	HNO_3	11	4	15	0	70	5

carbon support. The procedure has also been widely used in the preparation of metal colloids for homogeneous catalysis [41–43] as well as for heterogeneous catalysis [44–46]. In both the cases, nano-sized and well-dispersed metal colloids can be formed and stabilized in aqueous solution with the existence of polymer. Gold core and palladuim shell bimetallic clusters protected by polymers have also been prepared by an alcohol-reduction method [47].

In this communication, a nano-sized Pt–Ru/C catalyst has been produced using a modified alcohol-reduction method in which a small amount of Nafion is introduced during the preparation step. Addition of Nafion into the catalytic layer is believed to enhance the activity of Pt–Ru catalysts for the electro-oxidation of methanol by acting as a better dispersing agent and by increasing the ionic (protonic) conductivity. Earlier studies revealed that Nafion could be introduced into the catalyst layer by the deposition on top of the nanoparticles [48], by deposition both above and below the nanoparticles [49], or by mixing into nanoparticle ink [50]. The present study examines the influence of Nafion addition during the catalyst preparation step. The activities of the prepared Pt–Ru/C catalysts towards methanol oxidation were monitored and compared with that of standard Pt–Ru/C (E-TEK 40) catalyst.

2. Experimental

2.1. Chemicals

Hydrogen hexachloroplatinate ($H_2PtCl_6{\cdot}H_2O$, Acros), ruthenium chloride ($RuCl_3$, Acros), methanol (99.8%, Acros), sulfuric acid (97%, Acros) and Nafion® (5 wt.%, Aldrich) were used as-received. Solutions were made with de-ionized water (Millipore, Milli RO60). Commercial Vulcan XC-72 was used as a carbon support. Vulcan XC-72 was treated with HNO_3 prior to use.

2.2. Catalyst preparation and characterization

Various carbon supported Pt–Ru electrocatalysts (MEC-01, MEC-02, MEC-03 and MEC-04) were synthesized by the alcohol-reduction method employing methanol as a reducing agent. To the mixture of H_2PtCl6, $RuCl_3$ various portions of water, Vulcan XC-72 and 5 wt.% Nafion solution (ratio of Nafion solution to catalyst was kept at 1:3) were added and the pH of the mixture was adjusted to 11. After 4 h of stirring, various portions of methanol were added while keeping the volume of water and methanol solvent mixture constant for all the compositions. The resulting mixture was stirred at 70 °C for 5 h, washed with de-ionized water and filtered. The filtrate was analyzed for Pt and Ru with inductively coupled plasma atomic emission spectroscopy (ICP-AES). The results disclosed that most of the Pt and Ru was adsorbed on the carbon support. The catalyst powders after filtration were dried in an oven at 60 °C. The detailed preparation conditions were summarized in Table 1.

Powder X-ray diffraction (XRD) patterns for these catalysts were obtained on a diffractometer (Rigaku Dmax-B, Japan) using a Cu Kα source that was operated at 40 kV and 100 mA. The X-ray diffractograms were obtained at a scan rate of $0.05^\circ\,s^{-1}$ for 2θ values between 20° and 90°. Transmission electron microscopy (TEM) examination was performed on JEOL JEM-1010 microscope that operated at an accelerating voltage of 200 kV. Specimens were prepared by ultrasonically suspending the catalyst powders in ethanol, applying the specimen to a copper grid, and drying in air.

X-ray absorption spectroscopy measurements on in-house prepared MEC-01 and E-TEK 40 Pt–Ru/C catalysts were performed at the National Synchrotron Radiation Research Center (NSRRC), Hsinchu, Taiwan. The storage ring was operated with 1.5 GeV energy with beam currents of 100 to 200 mA. A Si(1 1 1) monochromator was used and was detuned by 10% to reject higher harmonics. Three ionization chambers, optimized for the Pt L_{III}-edge, were used in series to measure the intensities of the incident beam (I_0), the beam transmitted by the sample (I_t) and the beam subsequently transmitted by a Pt foil (I_r). The Pt foil was used as a reference.

Standard procedures were followed to analyze the Extended X-ray absorption fire structure (EXAFS) data. First, the raw absorption spectrum in the pre-edge region was fitted to a straight line and the background above the edge was fitted with a cubic spline. The EXAFS function, χ, was obtained by subtracting the post-edge background from the overall absorption and then normalized with respect to the edge jump step. The normalized $\chi(E)$ was transformed from energy space to k-space, where 'k' is the photoelectron wave vector. The $\chi(k)$ data was k^3-weighted and $k^3\chi(k)$ data in the k-space from 3.6 to 17.6 $Å^{-1}$ was Fourier transformed (FT) to r-space.

2.3. Electrochemical half-cell measurements and impedance analysis

Half-cell performance tests were performed in a three-electrode cell. A Pt wire and a saturated calomel electrode (SCE) were used as counter electrode and reference electrode, respectively. All the potentials in this paper are reported with respect to the standard hydrogen electrode (SHE). The working electrode was prepared as follow. The catalyst powder was dispersed in 5 wt.% Nafion® and isopropanol solution by keeping the ratio of catalyst to Nafion® at 1:3. From this solution, slurry containing approximately 1.87–2 $mg_{Pt–Ru}$ was dispersed on carbon cloth and dried at 75 °C for 1 min. The electrolyte solution contained 0.5 M H_2SO_4 and various concentrations of CH_3OH and was prepared with de-ionized water. A potentiostat (AUTO LAB, eco chemie, PGSTAT 20) was used for all the half-cell measurements. An electrochemical cell that consisted of a Pt–Ru/C catalyst pressed on Au ring as the working electrode (which was situated in a special Teflon holder), a saturated calomel electrode (SCE) as the reference electrode, and a Pt wire as the counter electrode was connected to Solartron 1260 & 1286 Impedance analyzer for electrochemical impedance spectroscopy analysis. The impedance of the working electrode in methanol concentrations of 5–50% was measured. The impedance spectra were obtained at frequencies between 100 kHz and 0.01 Hz. The amplitude of the sinusoidal potential signal was 10 mV.

3. Results and discussion

3.1. Structure of Pt–Ru/C catalysts

The XRD patterns of various in-house prepared catalysts are shown in Fig. 1. The wide peak near $2\theta = 25^\circ$ corresponds to diffraction of the carbon support. The diffraction peaks in the Pt–Ru catalyst curves match the (1 1 1), (2 0 0), (2 2 0), and (3 1 1) characteristics of a platinum fcc structure, but are shifted slightly to higher 2θ values. There are also no observable lines in the XRD scans that correspond to those of tetragonal RuO_2 and of the hcp structure of pure ruthenium. If the homogeneous solid-solution of Pt–Ru is not formed, then the XRD spectra of pure Ru in an hcp structure would be observed in the scan. The increase in 2θ values corresponds to a decrease in the lattice constants due to the incorporation of Ru atoms. Such incorporation in the fcc structure of platinum indicate the formation of Pt–Ru alloy in the catalyst [51].

The X-ray diffraction pattern for the in-house prepared catalyst MEC-01 was compared with the commercial E-TEK 40 Pt–Ru/C catalyst, as shown in Fig. 2. The average particle size was determined using the peak associated with the (2 2 0) plane of fcc Pt by using Scherrer's equation [52], and see Table 2. It is believed that in the (2 2 0) peak region there are no reflection signals associated with the carbon support. The dispersion of metal particles in the carbon support was investigated by TEM for Pt–Ru/C catalysts. The TEM images

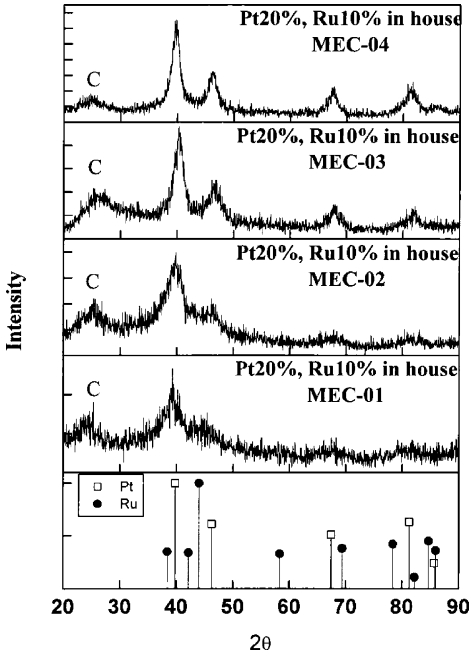

Fig. 1. XRD patterns of in-house prepared Pt–Ru/C catalyst powders.

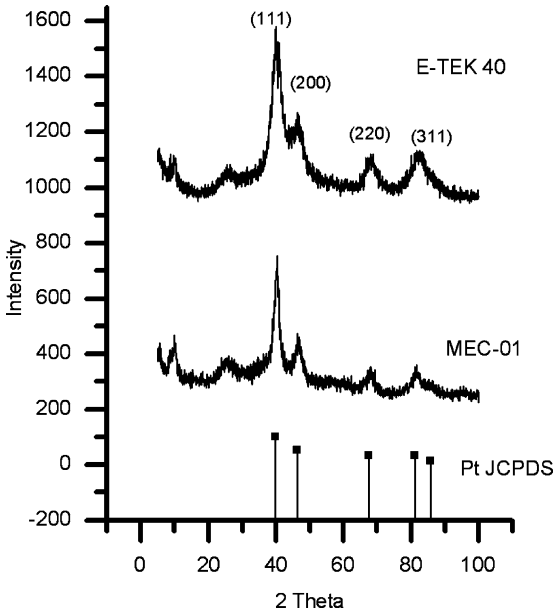

Fig. 2. Comparison of XRD patterns of MEC-01; E-TEK 40 and Pt JCPDS file (04-802).

Table 2
Particle sizes of in-house prepared Pt–Ru/C catalysts and E-TEK 40 Pt–Ru/C

Catalyst	Nafion (μL)	Methanol (mL)	Particle size (nm), TEM	Particle size (nm), XRD
MEC-01	1716	15	3–4	3.3
MEC-03	1716	25	3–15	–
MEC-04	0	15	5–7	–
E-TEK 40	0	–	2–3	2.4

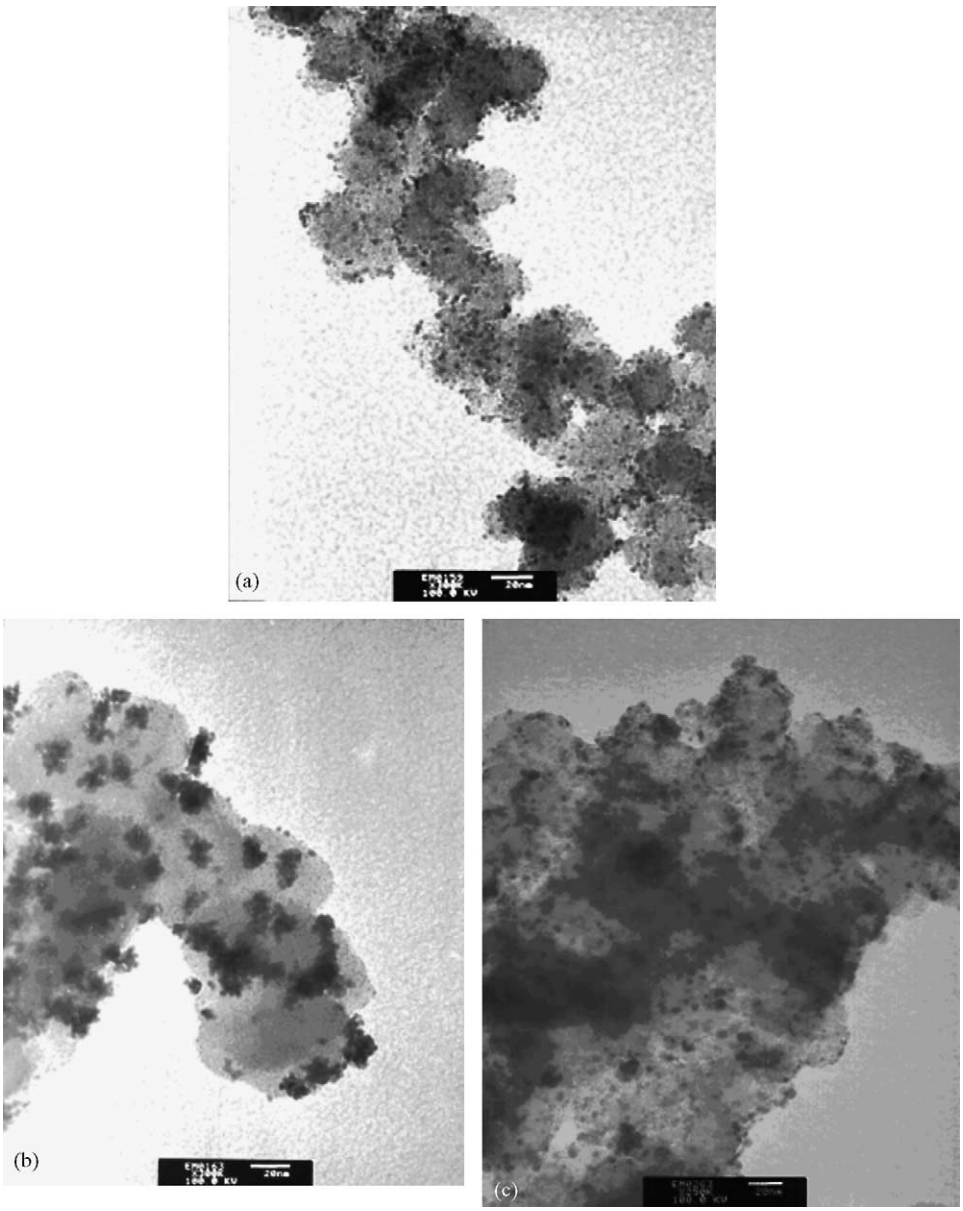

Fig. 3. TEM images of in-house prepared Pt–Ru/C catalysts. (a) MEC-01, (b) MEC-03 and (c) MEC-04.

of in-house prepared Pt–Ru/C catalysts shown in Fig. 3(a)–(c) reveal that metal particles of high contrast are well dispersed over the surface of the carbon. The standard Pt–Ru/C (E-TEK 40) catalyst shows a similar dispersion pattern over the carbon support (Fig. 4) when compared with the in-house prepared Pt–Ru/C catalyst MEC-01 (Fig. 3(a)). The addition of Nafion facilitates the dispersion of Pt–Ru particles on the carbon support. The average particle sizes of the in-house prepared catalysts are given in Table 2. This found that the catalyst prepared with Nafion addition (MEC-01, 3–4 nm) has a smaller particle size than that of catalyst prepared without Nafion (MEC-04, 5–7 nm). Probably the addition of Nafion during the preparation stage results in the controlled reduction of metal ions to form catalysts with lesser particle sizes. The addition of Nafion eliminates the use of stabilizers, which are commonly used to prevent cluster agglomeration [53–55]. Even though the addition of stabilizers prevents agglomeration and coalescence of the metal particles on the supports, their removal prior to the electrochemical measurements require complex procedures [56]. The addition of Nafion in the present investigation serves a dual advantageous role, namely: Nafion disperses well the catalyst particles on the carbon support, Nafion can also be used to control the size of the Pt–Ru particles formed. There is, however, a difference in particle size between the catalysts prepared with the same Nafion content (see Table 2). The catalyst produced with a low reducing agent concentration has a lower particle size (MEC-01, 3–4 nm), whereas the catalyst prepared with a high reducing agent concentration has a large particle size (MEC-03, 3–15 nm). With increasing concentration of reducing agent

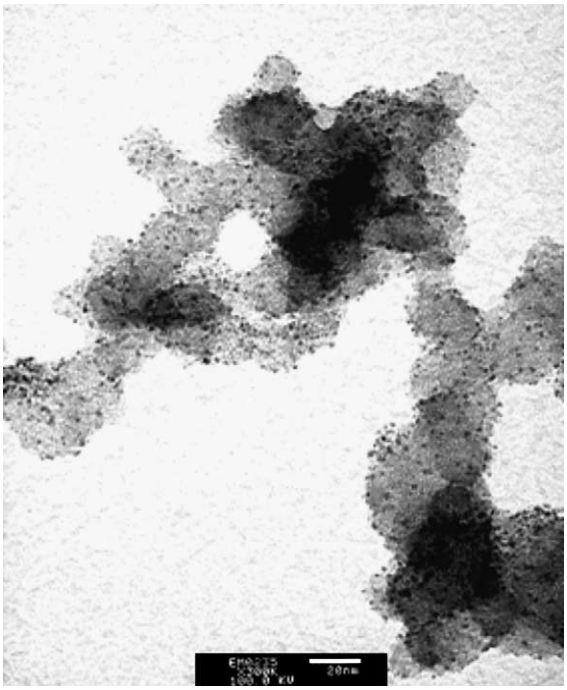

Fig. 4. TEM image of Pt–Ru/C (E-TEK 40) catalyst.

from MEC-01 to MEC-03, the driving force for the reduction increases. This causes particle agglomeration and results in the formation of catalysts with large particle sizes.

3.2. Electrochemical half-cell measurements

The reactivities of the in-house prepared Pt–Ru/C catalysts (MEC-01, MEC-02 and MEC-03) and standard Pt–Ru/C (E-TEK 40) catalyst towards methanol electro-oxidation were evaluated by performing half-cell measurements on the catalysts at 40 °C with varying concentrations of methanol. The results are presented in Fig. 5. The potential was swept between 0 and 1.0 V at 0.07 mV s^{-1}. The mass activities of both in-house prepared and commercial E-TEK 40 evaluated from Fig. 5(a)–(d) are listed in Table 3. For the catalysts MEC-01 and MEC-02 (Fig. 5(a) and (b)) at potentials above 0.35 V, the mass activity increases slightly with increase in methanol concentrations from 5 to 35%, and there after they start to decrease. The same pattern was observed for the standard Pt–Ru/C (E-TEK 40) catalyst (Fig. 5(d)). For the catalyst MEC-03, however, the mass activity decreases with increase in methanol concentration from 5 to 35%, and then starts to increase (Fig. 5(c)). The onset of methanol oxidation for MEC-01 for 5% methanol concentration (0.325 V), which is low compared with the onset potential for the standard Pt–Ru/C (E-TEK 40) catalyst (0.35 V versus NHE). The onset potential is defined as the potential at which 5% of the maximum current density at 0.7 V (minus the double-layer capacity) is reached [57]. It is well known that a lower onset potential for methanol oxidation has to be used for higher electrocatalytic activity. Both Leger and coworkers [57] and

Table 3
Mass activity (mA mg^{-1}) of various Pt–Ru/C catalysts at 40 °C and at various methanol concentrations calculated from anode current–potential curves of Fig. 5

Catalyst	Voltage (V)	Mass activity (mA mg^{-1})			
		5% CH_3OH	15% CH_3OH	35% CH_3OH	50% CH_3OH
MEC-01	0.4	1.62	3.11	2.67	2.48
MEC-01	0.6	10.95	15.38	14.37	12.1
MEC-01	0.8	22.79	31.14	29.7	25.22
MEC-02	0.4	0.04	0.07	0.11	0.11
MEC-02	0.6	1.16	2.25	3.05	2.72
MEC-02	0.8	4.38	7.32	9.38	7.97
MEC-03	0.4	1.82	1.65	1.22	1.97
MEC-03	0.6	11.3	9.97	7.86	8.45
MEC-03	0.8	23.1	20.6	17.05	18.42
E-TEK 40	0.4	0.55	2.48	2.74	2.01
E-TEK 40	0.6	5.56	17.37	17.95	14.27
E-TEK 40	0.8	7.98	35.7	38.61	29.68

Watanabe and coworkers [58] have used the variation in onset potential of methanol oxidation to probe the enhanced catalytic activity of Pt–Ru catalysts over a Pt catalyst. In present studies, it has been found that the onset potential for methanol oxidation on the in-house prepared catalyst (MEC-01) is significantly lower than that on standard E-TEK 40 Pt–Ru/C catalyst for all methanol concentrations studied (Fig. 6). This could be due to surface structural variations in the in-house prepared catalyst, which makes the dissociation of water on Ru faster at low potentials and, thereby, the surface adsorbed hydroxides (Ru–OH) oxidize the CO (or organic) species that are adsorbed on neighboring Pt sites in accordance with the bifunctional mechanism [26,27].

The electrode performances of the in-house prepared Pt–Ru/C and standard Pt–Ru/C (E-TEK 40) catalysts are compared in Fig. 7. The results from current–potential curves reveal that the in-house prepared catalysts MEC-01 and MEC-03 give higher performance than the standard Pt–Ru/C (E-TEK 40) catalyst (Fig. 7(a)) for 5% methanol concentration. For 15% methanol at 0.4 V, which is technologically interesting for DMFC applications, the MEC-01 Pt–Ru/C catalyst is the most active, while at more positive potentials the E-TEK 40 Pt–Ru/C catalyst is the most active (Fig. 7(b)). Similar results are observed for 35 and 50% methanol concentrations, see in Fig. 7(c) and (d), respectively. The impedance results (Table 5) agree well with the current–potential data and reveal that at an electrode potential of 0.4 V, the MEC-01 Pt–Ru/C catalyst has a lower resistance than the E-TEK 40 catalyst at all methanol concentrations. The high catalytic activity of the MEC-01 catalyst may be attributed to a homogeneous dispersion of metal particles on the carbon support with narrow particle-size distribution. In addition, the presence of Nafion inside the catalytic layer the MEC-01 catalyst would have improved the performance over commercial catalyst.

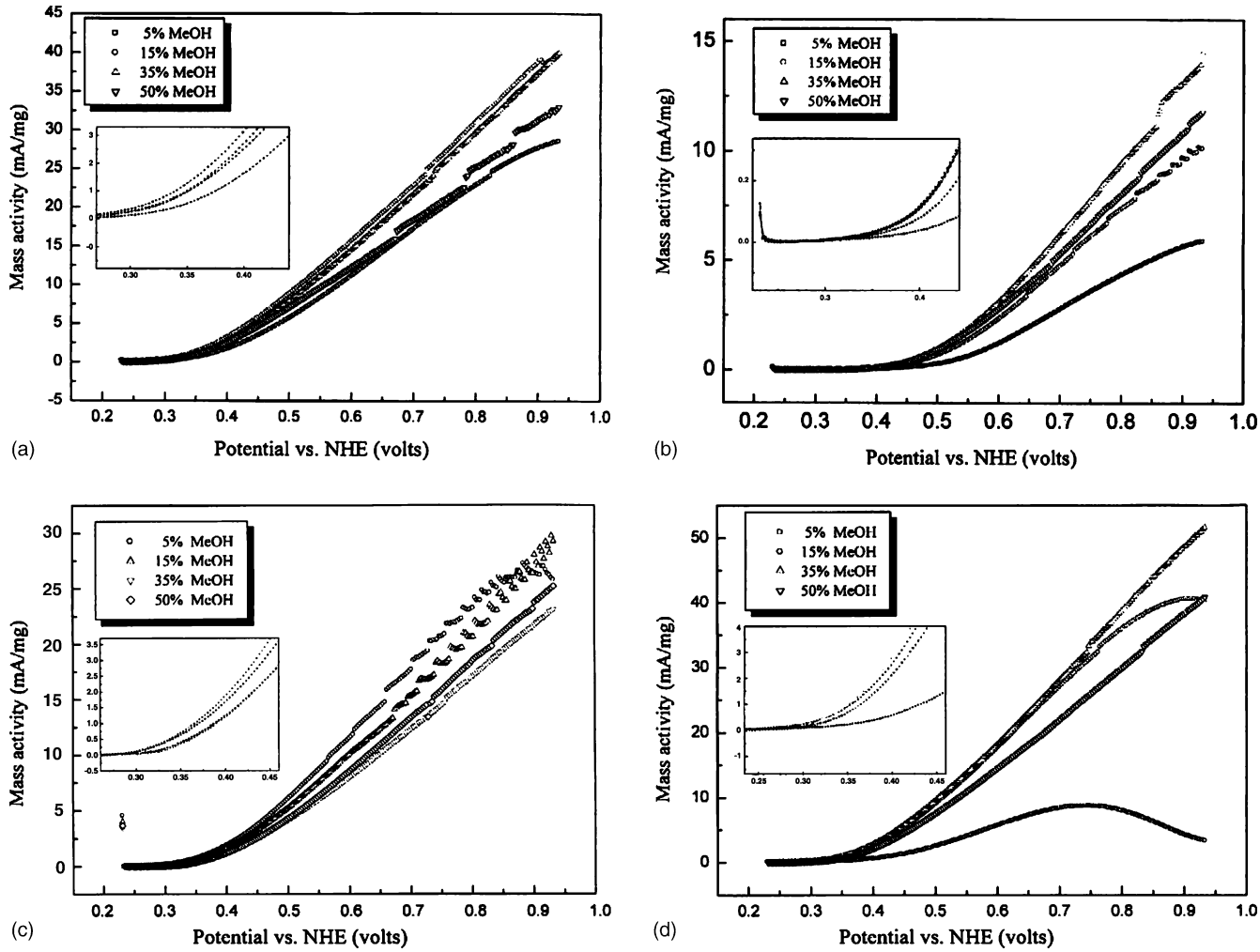

Fig. 5. Anodic current–potential curves of various Pt–Ru/C electrodes at 40 °C and in various methanol concentrations. (a) MEC-01, (b) MEC-02, (c) MEC-03 and (d) E-TEK 40.

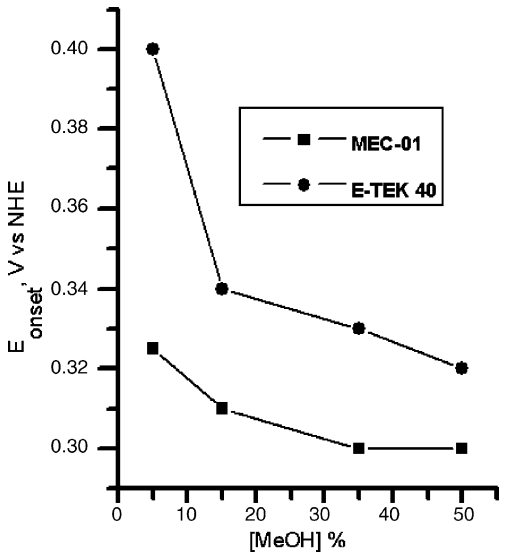

Fig. 6. Comparison of onset potential (E_{onset}) for methanol oxidation on in-house prepared Pt–Ru/C catalyst (MEC-01) and standard Pt–Ru/C catalyst (E-TEK 40) obtained from Fig. 5(a) and (d), respectively.

Conclusions about the electrocatalytic activity of Pt–Ru materials for methanol oxidation cannot be simply drawn from the characterization of as-prepared samples. X-ray absorption spectroscopy of the X-ray near edge structure (XANES) and the Extended X-ray absorption fine structure (EXAFS) is required for detailed characterization of the catalysts towards methanol oxidation.

3.3. X-ray absorption spectroscopy (XANES, EXAFS) measurements

Comparison of XANES features of the in-house prepared Pt–Ru/C catalyst (MEC-01) with the commercial E-TEK 40 catalyst at the Pt L_{III}-edge are presented in Fig. 8. It is seen that the MEC-01 catalyst has similar features to those of the commercial catalyst samples on the continuum, which indicates a similar environment for the Pt atoms in all samples. The white line at the Pt L_{III}-edge is an absorption threshold resonance; it is attributed to the electronic transitions from $2p_{3/2}$ to unoccupied states above the Fermi level and is sensi-

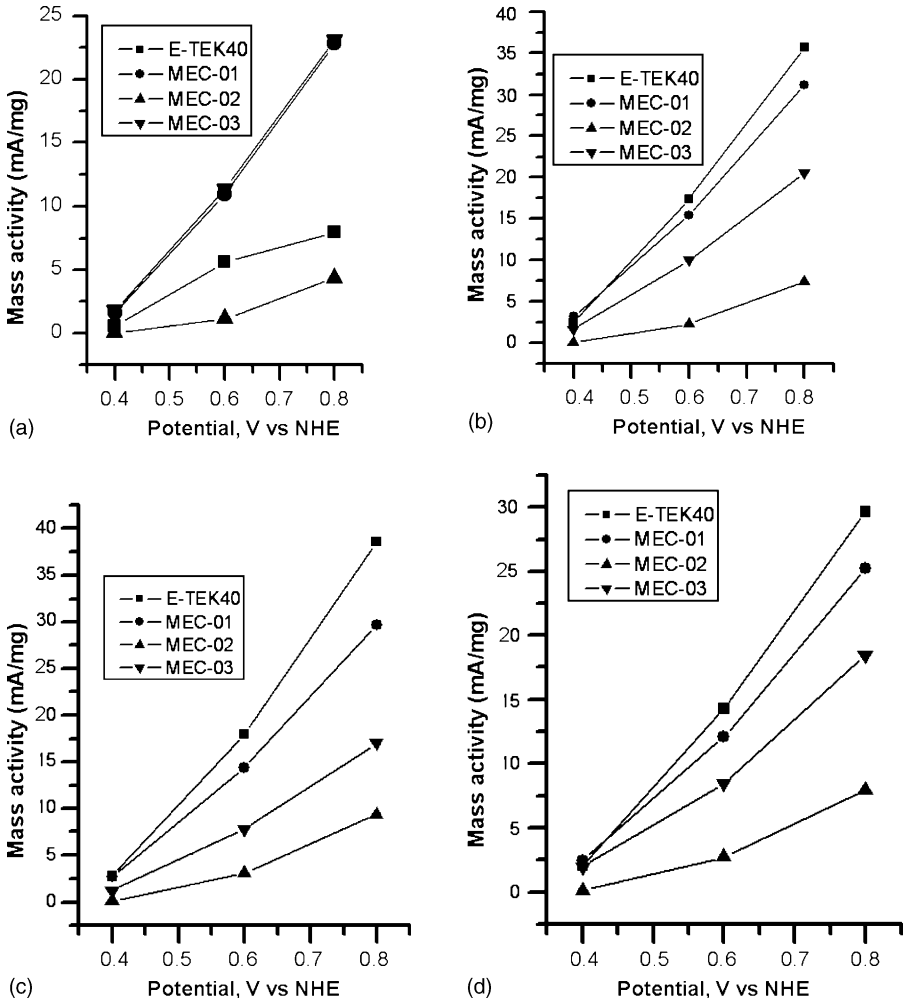

Fig. 7. Comparison of anode performance of various Pt–Ru/C electrodes at 40 °C in (a) 5% methanol, (b) 15% methanol, (c) 35% methanol and (d) 50% methanol.

Table 4
EXAFS fit parameters at Pt L_{III}-edge of MEC-01 and E-TEK 40 Pt–Ru/C catalysts

Sample	Shell	Calculated parameters				$S_0^2 = 0.05$
		N	R (Å)	$\Delta\sigma_j^2$ (Å^2)	ΔE_0 (ev)	R factor
MEC-01 (20% Pt, 10% Ru)	Pt–Ru	1.7 (0.5)	2.702 (0.010)	0.0047 (0.0014)	4.8 (2.0)	0.001
	Pt–Pt	6.4 (0.6)	2.746 (0.005)	0.0065 (0.0004)	5.5 (0.9)	
E-TEK (26.67% Pt, 13.33% Ru)	Pt–Ru	1.87 (0.2)	2.707 (0.003)	0.0052 (0.0002)	3.7 (0.9)	0.005
	Pt–Pt	6.2 (0.3)	2.745 (0.002)	0.0070 (0.0001)	6.2 (0.6)	

tive to changes in electron occupancy in the valence orbitals of the absorber [59]. Considerable differences are observed in the white line region between the prepared catalyst with those of commercial catalysts. The white line area is increased in the case of MEC-01, which signifies an increase in the d-band vacancies in Pt as a result of electron transfer from Pt or Ru caused by bimetallic interactions in the prepared catalyst. When the electron density is lower at Pt, there is a possibility of weakened CO adsorption and hence a higher methanol oxidation rate. This may be the reason for the superior performance of MEC-01 over E-TEK 40 at 5% methanol concentration. At higher methanol concentrations, however, the weakening of CO may be decreased in MEC-01 compared with E-TEK 40, and hence there is a decrease in methanol oxidation performance. A systematic investigation is required to confirm this assumption and will be addressed in future work. Lin et al. [60] have related the enhanced intensity of the white line area of the prepared Pt–Ru/C catalyst to the higher performance of their prepared Pt–Ru/C catalyst compared with that of a commercial Pt–Ru/C catalyst. Page et al. [61]

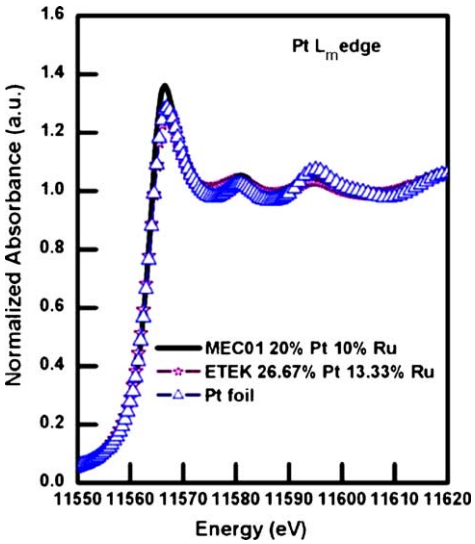

Fig. 8. Pt L_{III}-edge XANES spectra of MEC-01, E-TEK 40 Pt–Ru/C catalysts and Pt foil.

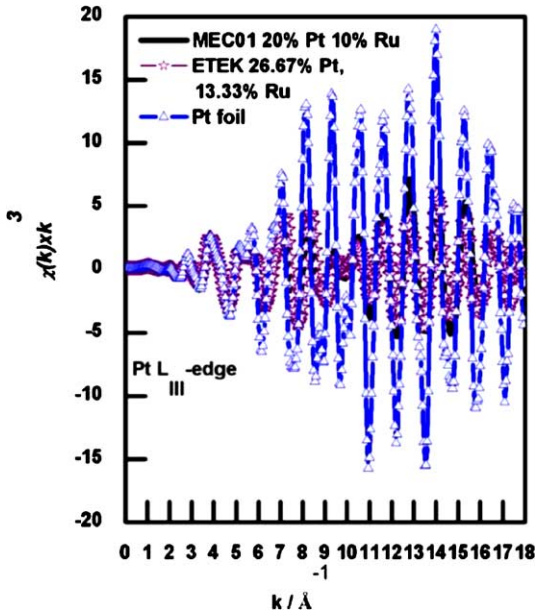

Fig. 9. k^3-Weighted EXAFS spectra of Pt foil, MEC-01, E-TEK 40 Pt–Ru/C catalysts.

have found a reduced white line for Pt–Ru/C catalysts compared with a commercial Pt–Ru/C catalyst and have related this observation in prior to the electrochemical performance of the prepared catalyst. Normalized EXAFS (k^3-weighted) data for the Pt foil, MEC-01 catalyst and E-TEK 40 Pt–Ru/C electrocatalyst are shown in Fig. 9. The three data sets exhibit similarity even at higher k values. The k^3-weighted EXAFS data were Fourier transformed, as shown in Fig. 10. For the Pt–Ru/C catalysts, splitting of the peak corresponding to the first coordination shell is observed and is caused by the interference between backscattering from Pt and Ru neighbors. This phenomenon has been ascribed to the formation of a real Pt–Ru alloy [62,63]. It is necessary, however, to confirm the presence of bimetallic interaction from Ru K-edge but due to energy constraints at NSRRC, Taiwan, only data recorded at Pt L_{III}-edge have been examined on MEC-01 and commercial Pt–Ru/C samples. EXAFS parameters such as coordination number (N), bond distance (R), Debye–Waller factor ($\Delta\sigma_j^2$) and energy shift (ΔE_0) are listed in Table 4. The Pt–Pt as well as Pt–Ru coordination numbers of both MEC-01 and E-TEK 40 Pt–Ru/C catalysts are nearly the same and this indicates that the catalysts may have similar structures. For all samples, the total Pt–Pt and Pt–Ru coordination numbers are

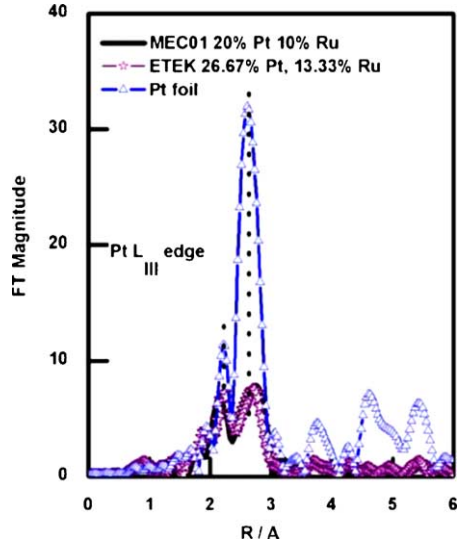

Fig. 10. Fourier transformed EXAFS spectra of MEC-01, E-TEK 40 Pt–Ru/C catalysts and Pt foil.

Table 5
Comparison of fitting parameters using equivalent circuit of Fig. 12 for E-TEK 40 and MEC-01 Pt–Ru/C catalyst electrodes at 40 °C, 0.4 V and various methanol concentrations

Electrode	MeOH (%)	R_s (mg Ω)	R_1 (mg Ω)	CPE_1-T (F mg^{-1})	CPE_1-P (F mg^{-1})	R_2 (mg Ω)	CPE_2-T (F mg^{-1})	CPE_2-P (F mg^{-1})
E-TEK 40	5	0.867	0.454	0.0006	0.73	139.49	0.0386	0.93
	15	1.046	0.469	0.0005	0.76	73.797	0.0378	0.92
	35	1.25	0.485	0.001	0.7	37.026	0.0362	0.91
	50	1.658	0.714	0.0072	0.54	38.811	0.0362	0.93
MEC-01	5	0.045	0.121	0.0018	0.66	26.18	0.0691	0.9
	15	0.061	0.176	0.0035	0.61	17.688	0.0667	0.92
	35	0.704	0.187	0.0033	0.61	14.74	0..0655	0.9
	50	0.913	0.286	0.034	0.43	13.618	0.0794	0.95

considerably smaller than that in bulk Pt ($N = 12$), and this is consistent with the formation of highly dispersed and small particle Pt-based alloys.

3.4. Electrochemical impedance spectroscopy analysis

ac impedance spectroscopy is a direct method for the study of various electrochemical processes involved in the operation of DMFCs. Nyquist plots for the standard Pt–Ru-C (E-TEK 40) catalyst and in-house prepared Pt–Ru-C (MEC-01) catalyst at various methanol concentrations at 40 °C and at bias potential of 0.4 V are were shown in Fig. 11(a) and (b), respectively. The Nyquist plots agree well with the experimentally observed plots when the equivalent circuit shown in Fig. 12, which has been based on the discussion the impedance in PEMFCs [64] and modified to fit the present three-electrode cell arrangement, is used to model the impedance behaviour of Pt–Ru/C electrodes. R_s is the solution resistance, R_1 is the interfacial resistance between the catalyst and the Au ring in parallel with a constant phase element (CPE_1) and R_2 is the charge-transfer resistance due to methanol oxidation kinetics in parallel with a constant phase element (CPE_2). The fitting parameters using this equivalent circuit are shown in Table 5. The solution resistance (R_s) increases in small amounts with increase in methanol concentration both for the standard Pt–Ru/C catalyst (E-TEK 40) and for the in-house prepared MEC-01 Pt–Ru/C catalyst, but the extent of the increase is small. Even though the solution resistance is a bulk property of the electrolyte solution and independent of the interfacial properties of the electrode, it is reasonable to expect a small increase as the concentration of methanol is increased. The interfacial resistance between the catalyst and the Au ring (R_1) also shows a small increase for both catalysts. The increase in methanol adsorption on the catalyst with concentration will probably increase the interfacial resistance to a small extent. The impedance spectra for the E-TEK 40 catalyst shown in Fig. 11(a) display a semicircle in the low-frequency region. The magnitude of this semicircle decreases as the methanol concentration is increased from 5 to 35%, while the corresponding change-transfer resistance (R_2) decreases and then slightly increases for 50% methanol. It is well known that the magnitude of the semicircle is related to the resistance due to the methanol electro-oxidation kinetics [65,66]. The extent of the decrease in resistance indicates the increasing driving force for the methanol oxidation process. The data in Fig. 11(a) and Table 5 clearly indicate that the E-TEK 40 catalyst has a lower resistance at 35% methanol and a higher resistance at 50% methanol. The impedance results for the E-TEK 40 electrode at 0.4 V are in agreement with the polarization curve at 0.4 V, which suggests that the mass activity increases up to 35% methanol concentration and then decreases. Studies on the MEC-01 Pt–Ru/C catalyst show that the resistance values decrease with increasing methanol concentration (Fig. 11(b) and Table 5) and all the values are well below those of E-TEK 40. The specific resistance of E-TEK 40 and MEC-01

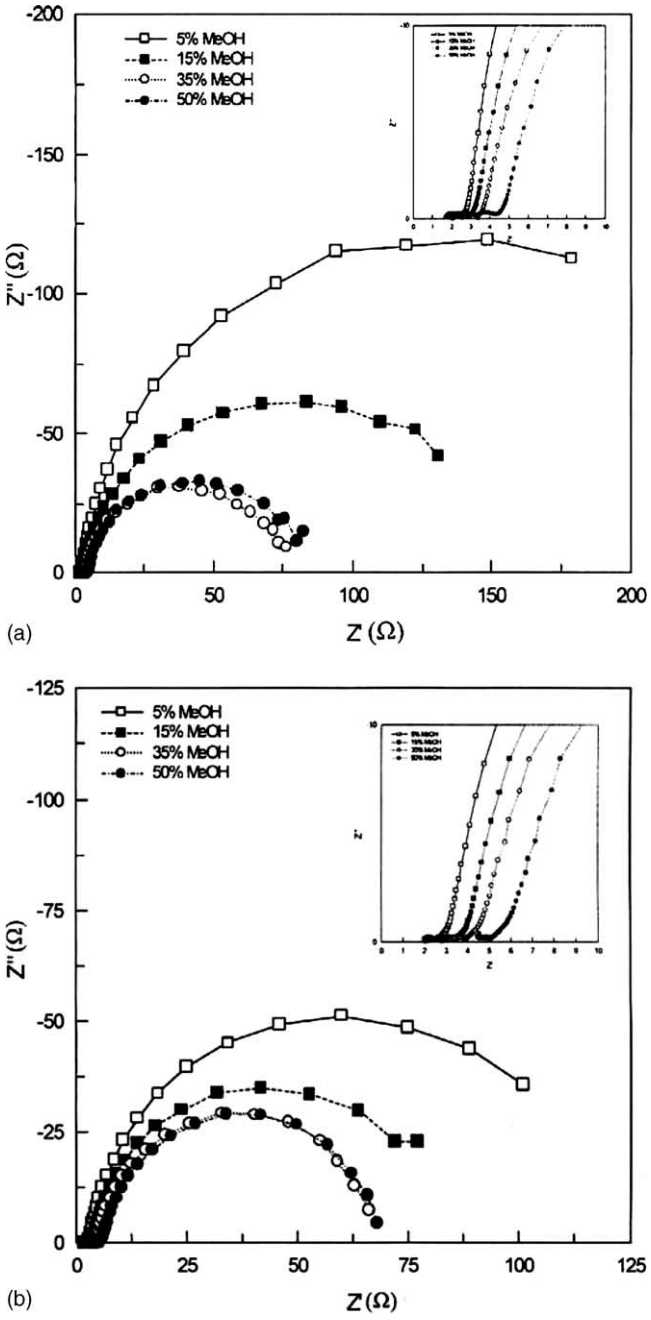

Fig. 11. Nyquist diagrams at of 0.4 V and of 40 °C. (a) E-TEK 40 catalyst, (b) in-house prepared MEC-01 Pt–Ru/C catalyst.

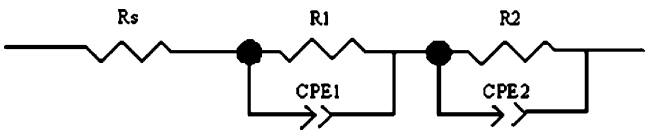

Fig. 12. Equivalent circuit for evaluation of impedance spectra measured during electro-oxidation of methanol on Pt–Ru/C catalysts.

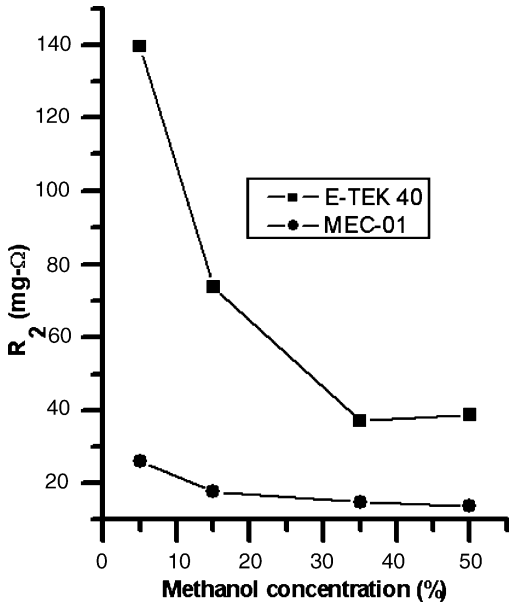

Fig. 13. Relationship between specific resistance (R_2) and methanol concentration of E-TEK 40 and MEC-01 Pt–Ru/C catalysts.

catalysts is plotted against various methanol concentrations in Fig. 13. For all methanol concentrations, the commercial E-TEK 40 catalyst exhibits higher specific resistance. Half-cell polarization and impedance analysis demonstrate that the Pt–Ru/C (MEC-01) gives a showed higher performance than the standard Pt–Ru/C (E-TEK 40) catalyst.

4. Conclusions

Well-dispersed Pt–Ru particles deposited on a Vulcan XC-72 carbon support via the alcohol-reduction method for methanol electro-oxidation. The addition of small amounts of Nafion in the catalyst preparation step enhances the electrocatalytic activity compared with that of commercial Pt–Ru/C (E-TEK 40) catalyst.

Acknowledgements

The financial support from the National Science Council (NSC 92-2811-E-011-001), the Education Ministry (EX-92-E-FA09-5-4), the National Synchrotron Radiation Research Center (NSRRC), Hsinchu, and the National Taiwan University of Science and Technology, Taiwan, Republic of China is great fully acknowledged.

References

[1] M.P. Hogarth, G.A. Hards, Platinum Met. Rev. 40 (1996) 150.
[2] K. Kordesch, G. Simader, Fuel Cells and their Applications, VCH, Weinheim, 1996.
[3] L. Liu, C. Pu, R. Viswanathan, Q. Fan, R. Liu, E.S. Smotkin, Electrochem. Acta 43 (1998) 3657.
[4] X. Ren, M.S. Wilson, S. Gottesfeld, J. Electrochem. Soc. 143 (1996) L12.
[5] S.R. Narayanan, W. Chun, T.I. Valdez, B. Jeffries-Nakamura, H. Frank, S. Surampudi, G. Halpert, J. Kosek, C. Cropley, A.B. LaConti, M. Smart, Q. Wang, G. Surya Prakash, G.A. Olah, Program and abstracts, Fuel Cell Seminar (1996) 525.
[6] M. Baldauf, W. Preidel, Proceedings of the Symposium on Electrochemical Energy Conversion and Storage for Mobile Applications, Ulm, Germany, 1998.
[7] B.D. McNicol, D.A.J. Rand, K.R. Williams, J. Power Sources 83 (1999) 15.
[8] B.D. McNicol, J. Electroanal. Chem. 118 (1981) 71.
[9] R.G. Hockaday, M. DeJohn, C. Navas, P.S. Turner, H.L. Vaz, L.L. Vazul, Program and abstracts, Fuel Cell Seminar, Portland, OR (2000) 791.
[10] S.C. Kelly, G.A. Deluga, W.H. Smyrl, Electrochem. Solid-State Lett. 3 (1999) 407.
[11] A.S. Arico, P. Creti, P.L. Antonucci, V. Antonucci, Electrochem. Solid-State Lett. 1 (1998) 4.
[12] N.A. Hampson, M.J. Wilars, J. Power Sources 4 (1979) 191.
[13] M. Gotz, H. Wendt, Electrochim. Acta 43 (1998) 3637.
[14] H.A. Gasteiger, N. Markovic, P.N. Ross, E.J. Cairns, J. Phys. Chem. 97 (1993) 12020.
[15] A. Oliveira-Neto, J. Perez, W.T. Napporn, E.A. Ticianelli, E.R. Gonzalez, J. Brazil. Chem. Soc. 11 (2000) 39.
[16] K.L. Ley, R. Liu, C. Pu, Q. Fan, N. Leyarovska, C. Segre, E.S. Smotkin, J. Electrochem. Soc. 144 (1997) 1543.
[17] A.S. Arico, Z. Poltarzewski, H. Kim, A. Morana, N. Giordano, V. Antonucci, J. Power Sources 55 (1995) 159.
[18] B. Gurau, R. Viswanathan, R. Liu, T.J. Lafrenz, K.L. Ley, E.S. Smotkin, A. Sapienza, B.C. Chan, T.E. Mallouk, S. Sarangapani, J. Phys. Chem. B 102 (1998) 9997.
[19] E. Antolini, Mater. Chem. Phys. 78 (2003) 78.
[20] C. Lamy, J.M. Leger, in: A. Wieckowski (Ed.), Interfacial Electrochemistry: Theory, Experiment and Applications, Marcel Dekker, New York, 1999, p. 885.
[21] A. Arico, S. Srinivasan, V. Antonucci, Fuel Cells 1 (2001) 1.
[22] S. Wasmus, A. Kuver, J. Electroanal. Chem. 461 (1999) 14.
[23] M. Hogarth, T. Ralph, Platinum Met. Rev. 46 (2002) 146.
[24] H.A. Gasteiger, N.M. Markovic, P.N. Ross Jr., E.J. Cairns, J. Phys. Chem. 99 (1995) 16757.
[25] P.N. Ross Jr., in: J. Lipkowski, P.N. Ross (Eds.), Electrocatalysis, Wiley/VCH, New York, 1998, p. 43.
[26] M. Watanabe, S. Motoo, J. Electroanal. Chem. 60 (1975) 267.
[27] M. Watanabe, S. Motoo, J. Electroanal. Chem. 60 (1975) 275.
[28] H. Bonnemann, R. Brinkmann, P. Britz, U. Endruschat, R. Mortel, G. Feldmeyer, T. Schmidt, H. Gasteiger, R. Behm, J. New Mater. Electrochem. Syst. 3 (2000) 199.
[29] U. Paulus, U. Endruschat, G. Feldmeyer, T. Schmidt, R. Behm, J. Catal. 195 (2000) 383.
[30] E. Antolini, L. Giorgi, F. Cardellini, E. Passalacqua, J. Solid State Electrochem. 5 (2001) 131.
[31] A. Pozio, R. Silva, M. De Francesco, F. Cardellini, L. Giorgi, Electrochim. Acta 48 (2002) 255.
[32] A. Luna, G. Camara, V. Paganin, E. Ticianelli, E. Gonzalez, Electrochem. Commun. 2 (2000) 222.
[33] N. Fujiwara, Y. Shiozaki, T. Tanimitsu, K. Yasuda, Y. Miyazaki, Electrochemistry 70 (2002) 988.
[34] G. Che, B. Lakeshmi, E. Fisher, C. Martin, Nature 393 (1998) 346.
[35] E. Antolini, F. Cardellini, J. Alloys Compd. 315 (2001) 118.
[36] E. Steigerwalt, G. Deluga, D. Cliffel, C. Lukehart, J. Phys. Chem. B 105 (2001) 8097.
[37] C. Hills, N. Mack, R. Nuzzo, J. Phys. Chem. B 107 (2003) 2626.
[38] X. Zhang, K.Y. Chan, Chem. Mater. 15 (2003) 451.

[39] Y. Liu, X. Qiu, Z. Chen, W. Zhu, Electrochem. Commun. 4 (2002) 550.
[40] X. Wang, I.-M. Hsing, Electrochim. Acta 47 (2002) 2981.
[41] N. Toshima, K. Hirakawa, Polym. J. 31 (1999) 1127.
[42] D. Duff, T. Mallat, M. Schneider, A. Baiker, Appl. Catal. A: Gen. 133 (1995) 133.
[43] N. Toshima, M. Kuriyama, Y. Yamada, H. Hirai, Chem. Lett. (1981) 793.
[44] N. Toshima, K. Kushihashi, T. Yonezawa, H. Hirai, Chem. Lett. (1989) 1769.
[45] B. Zhao, N. Toshima, Chem. Express 5 (1990) 721.
[46] N. Toshima, J. Macromol. Sci. Chem. A 27 (1990) 1225.
[47] N. Toshima, M. Harada, Y. Yamazaki, K. Asakura, J. Phys. Chem. 96 (1992) 9927.
[48] S.Y. Cha, W.M. Lee, J. Electrochem. Soc. 146 (1999) 4055.
[49] S.D. Thompson, L.R. Jordan, M. Forsyth, Electrochim. Acta 46 (2001) 1657.
[50] M. Sogaard, M. Odgaard, E.M. Skou, Solid State Ionics 145 (2001) 31.
[51] A.S. Arico, P. Creti, H. Kim, R. Mantegna, N. Giordano, V. Antonucci, J. Electrochem. Soc. 143 (1996) 3047.
[52] A.R. West, Solid State Chemistry and Its Applications, Wiley, New York, 1984.
[53] H. Bonnemann, W. Brijoux, R. Brinkmann, E. Dinjus, T. Joussen, B. Korall, Angew. Chem. 103 (1991) 1344.
[54] H. Bonnemann, G. Braun, W. Brijoux, R. Brinkmann, A. Schulze-Tilling, K. Seevogel, K. Siepen, J. Organomet. Chem. 520 (1996) 143.
[55] M.T. Reetz, S. Quaiser, R. Breinbauer, B. Tesche, Angew. Chem. 107 (1995) 2956.
[56] U.A. Paulus, U. Endruschat, G.J. Feldmeyer, T.J. Schmidt, H. Bonnemann, R.J. Behm, J. Catal. 195 (2003) 383.
[57] C. Roth, N. Martz, F. Hahn, J.-M. Leger, C. Lamy, H. Fuess, J. Electrochem. Soc. 149 (2002) E433.
[58] N. Wakabayashi, H. Uchida, M. Watanabe, Electrochem. Solid-State Lett. 5 (2002) E-62.
[59] J.A. Horsely, J. Chem. Phys. 76 (1982) 1451.
[60] S.D. Lin, T.C. Hsiao, J.R. Chang, A.S. Lin, J. Phys. Chem. B 103 (1999) 97.
[61] T. Page, R. Johnson, J. Hormes, S. Noding, B. Rambabu, J. Electroanal. Chem. 485 (2000) 34.
[62] J. McBreen, S. Mukerjee, J. Electrochem. Soc. 142 (1995) 3399.
[63] M.S. Nasher, A.I. Frenkel, D.L. Adler, J.R. Shapley, R.G. Nuzzo, J. Am. Chem. Soc. 119 (1997) 7760.
[64] M. Ciureanu, S.D. Mikhailenko, S. Kaliaguine, Catal. Today 82 (2003) 195.
[65] J.T. Muller, P.M. Urban, J. Power Sources 75 (1998) 139.
[66] J.T. Muller, P.M. Urban, W.F. Holderich, J. Power Sources 84 (1999) 157.